

Fully automatic computer-aided mass detection and segmentation via pseudo-color mammograms and Mask R-CNN

Hang Min¹, Devin Wilson¹, Yinhuang Huang¹, Samuel Kelly¹, Stuart Crozier¹, Andrew P Bradley^{1,2}, Shekhar S. Chandra¹

¹*School of Information Technology and Electrical Engineering, University of Queensland, Australia.*

²*Science and Engineering Faculty, Queensland University of Technology, Australia.*

Purpose: To propose pseudo-color mammograms that enhance mammographic masses as part of a fast computer-aided detection (CAD) system that simultaneously detects and segments masses without any user intervention.

Methods: The proposed pseudo-color mammograms, whose three channels contain the original grayscale mammogram and two morphologically enhanced images, are used to provide pseudo-color contrast to the lesions. The morphological enhancement ‘sifts’ out the mass-like mammographic patterns to improve detection and segmentation. We construct a fast, fully automated simultaneous mass detection and segmentation CAD system using the colored mammograms as inputs of transfer learning with the Mask R-CNN which is a state-of-the-art deep learning framework. The source code for this work has been made available online.

Results: Evaluated on the publicly available mammographic dataset INbreast, the method outperforms the state-of-the-art methods by achieving an average true positive rate of 0.90 at

0.9 false positive per image and an average Dice similarity index for mass segmentation of 0.88, while taking 20.4 seconds to process each image on average.

Conclusions: The proposed method provides an accurate, fully-automatic breast mass detection and segmentation result in less than half a minute without any user intervention while outperforming state-of-the-art methods.

Key words: Mammography, computer-aided detection, breast mass, morphological sifting, deep learning

I. Introduction

Breast cancer is one of the most frequently diagnosed cancers among women worldwide¹. Mammography has long been regarded as the primary tool for breast screening². During breast screening, the large volume of data generated can lead to fatigue and missed detections in human analysis. To assist radiologists and increase confidence of detection, computer-aided detection (CAD) systems have been developed as a ‘second pair of eyes’ in mammogram interpretation².

The identification of breast masses can be difficult due to the variation in size, shape and contrast to the background tissue³. Many conventional breast mass CAD systems contain a region proposal, a feature extraction and a classification stage⁴. These studies mainly rely on hand-crafted features to depict breast masses. However, it can be difficult to achieve a balance between discriminative power and robustness when using hand-crafted features⁵. Recent developments in deep learning (DL) based methods can provide more robust solutions to this problem. Various convolutional neural networks (CNNs) have been applied to breast mass detection and segmentation⁶⁻⁹. These methods learn meaningful features directly from the training data and have achieved promising results. However, some of these methods^{8,9} only focus on one task, either mass detection or segmentation. Recent studies^{6,7} are able to

generate both detection and segmentation results. However, false positive (FP) detections need to be manually removed before performing the segmentation task. Therefore, there is still a need for an end-to-end system that simultaneously detects and segments mammographic masses. It is also worth noting that CNNs can handle 3 channel (RGB) images, while mammograms are normally grayscale images. Appending two additional channels to the grayscale mammograms and transforming them into colored images may have the potential to improve the detection performance.

In this work, we introduce the concept of pseudo-color mammograms that renders mass-like patterns with color contrast with respect to the background. The pseudo-color mammogram is generated by appending two morphologically filtered mammograms (see section II.C) to the grayscale mammogram in two adjacent image channels as shown in Figure 1. To identify masses on pseudo-color mammograms, we adopt transfer learning with the Mask R-CNN due to the limited size of publicly available mammographic datasets. The Mask R-CNN is a recently proposed general framework for object detection and segmentation¹⁰. To the best of our knowledge, this is the first attempt to evaluate Mask R-CNN on mammographic mass detection and segmentation that achieves beyond the state-of-the-art performance. The proposed pseudo-color scheme paired with the Mask R-CNN deep learning framework provides an integrated solution to mammographic mass detection and segmentation that does not require any manual intervention or hand-crafted features and has runtimes per image less than half a minute. This work is evaluated on the publicly available INbreast dataset¹¹ and outperforms the state-of-the-art methods on identical evaluation sets. The source code for this work has been made available online¹².

II. Materials and methods

In this section, we introduce the dataset used for evaluation and provide a detailed technical explanation of the proposed method. As shown in Figure 1, the proposed method consists of a pre-processing, a pseudo-color image generation and a detection & segmentation stage using Mask R-CNN.

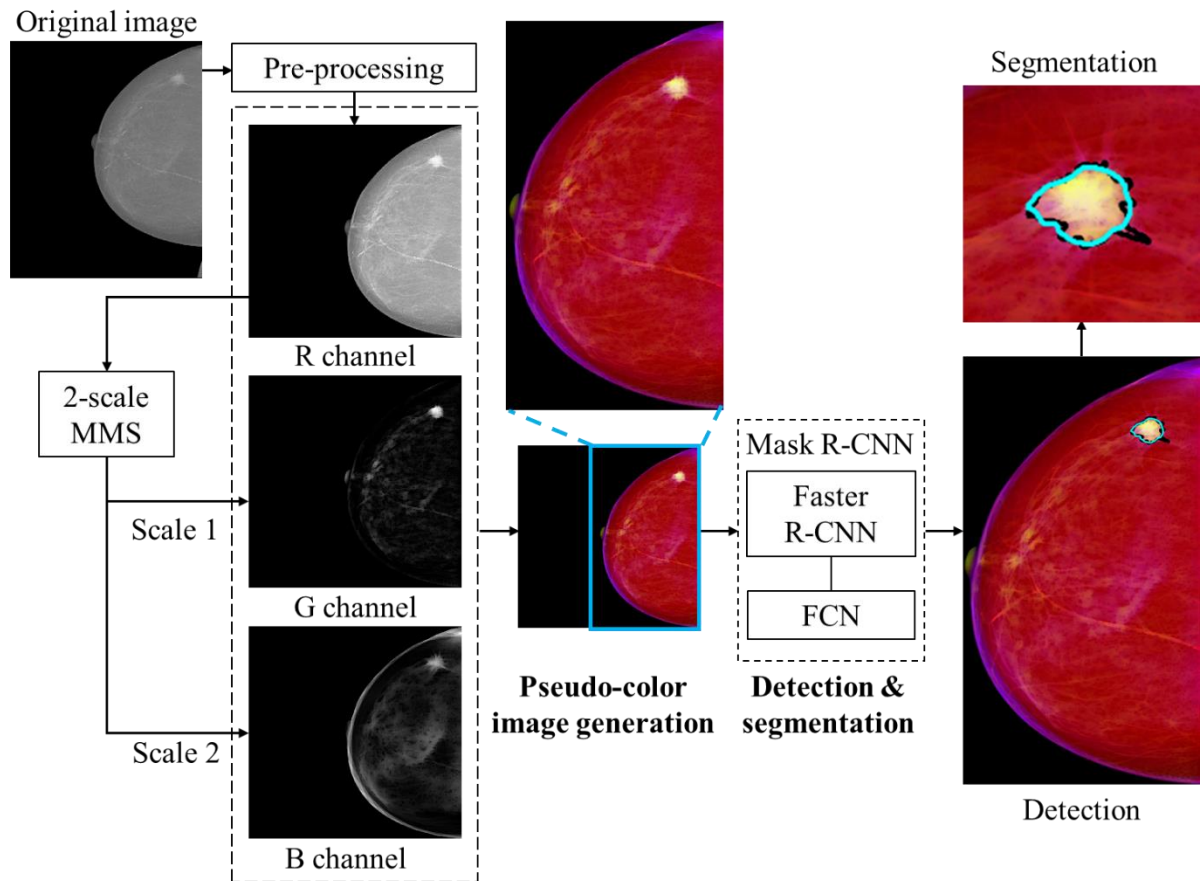


Figure 1. The diagram of the proposed method. MMS stands for multi-scale morphological sifting and FCN stands for fully convolutional network. The black outlines represent the annotation of the lesion and the cyan outlines represent the segmentation generated by the proposed method.

A. Datasets

The INbreast dataset¹¹ is used for evaluating the proposed method. This dataset is currently the largest publicly available full-digital mammographic dataset with mammograms precisely annotated⁶. It contains 115 cases with 410 mammograms. There are 116 breast masses in total, within the size range of $[15mm^2, 3689mm^2]$. The pixel size of the mammograms is $70\mu m$, and the bit depth is 14-bit.

B. Pre-processing

The breast region is extracted by thresholding and the redundant background is cropped away¹³. The mammogram is then normalized to 16-bit and padded into a square shape. To speed up the process, the mammogram is sub-sampled to 1/4 of its original size using the low-pass component of a two-level Daubechies 2 wavelet transform¹⁴.

C. Pseudo-color mammogram generation

In this stage, the mammogram is transformed into a pseudo-color image. This pseudo-color rendering scheme can enhance mass-like patterns selectively in each scale and add color contrast between the lesion and the background tissue when combining three channels. With the grayscale image in one of the three channels, the other two channels are filled in with two images generated by the multi-scale morphological sifter (MMS)¹³ as shown in Figure 1. The MMS algorithm uses oriented linear structuring elements (LSE) to extract patterns of interest that fit in the size range specified by the LSEs. Eq. (1) describes the morphological sifting (MS) on scale i ($i=1, \dots, I$), where an input image F is processed by two sets of morphological filters and ‘ \circ ’ stands for morphological opening. Each set of filters $L(M(i), \theta(n))$ contains N LSEs. M stands for the magnitude and $\{\theta(n) = n \times (180^\circ / N) \mid n = 0, 1, \dots, N-1\}$ stands for the orientation of each LSE. The magnitudes M_1 and M_2 are defined in Eq. (2, 3). On scale i , the MS is able to extract patterns whose

diameter is within the range of $[M_1(i), M_2(i)]$. Given the area range of the target for detection $[A_{\min}, A_{\max}]$, the magnitude range for the LSEs $[M_{\min}, M_{\max}]$ can be estimated as in Eq. (4), where P is the pixel size of the original image and R is the resizing factor in the pre-processing stage.

$$F_ms(i) = \sum_{n=0}^{N-1} \{F - [F \circ L(M_2(i), \theta(n))]\} \circ L(M_1(i), \theta(n)) \quad (1)$$

$$M_1(i) = M_{\min} \times (M_{\max} / M_{\min})^{(i-1)/I} \quad (2)$$

$$M_2(i) = M_{\min} \times (M_{\max} / M_{\min})^{i/I} \quad (3)$$

$$[M_{\min}, M_{\max}] = [2(A_{\min} / \pi)^{0.5} / PR, 2(A_{\max} / \pi)^{0.5} / PR] \quad (4)$$

In this work, two scales are used for the MMS ($I = 2$) and the size range of the lesions $[A_{\min}, A_{\max}]$ has been suggested in Moreira et al.¹¹. The two output images and the grayscale mammogram are linearly scaled to 8-bit. A pseudo-color image consists of the grayscale mammogram in the R (red) channel, the output image of MMS from scale 1 in the G (green) channel and the output image from scale 2 in the B (blue) channel as shown in Figure 1.

D. Applying Mask R-CNN

In this work, we adopt transfer learning with a pre-trained Mask R-CNN model, since the mammographic dataset is limited in size. The Mask R-CNN, as an extension of Faster R-CNN¹⁵, provides a general framework for simultaneous lesion detection and segmentation. It consists of the Faster R-CNN for object detection and a fully convolutional network (FCN)¹⁶ for a pixel-to-pixel segmentation. The Faster R-CNN uses a region proposal network to propose bounding box region candidates and then classifies these candidates into different categories¹⁵. The FCN runs in parallel to perform segmentation on the region candidates¹⁰.

The loss function of Mask R-CNN is $L = L_{cls} + L_{bbox} + L_{msk}$, where the classification loss L_{cls} and bounding box loss L_{bbox} were originally defined in study¹⁷. The mask loss L_{msk} is defined as the binary cross-entropy loss with a per-pixel sigmoid activation¹⁰.

E. Experiments

The proposed method is evaluated on the INbreast dataset. Here, we use the repeated random sub-sampling validation¹⁸. The dataset is randomly split into training, validation and testing sets five times, the same as previous studies^{6,13,19,20}. In pseudo-color image generation, the number of LSEs (N) in each scale is set to 18, the same as Min et al.¹³. The number of scales (I) is set to 2. The size range of the lesions $[A_{min}, A_{max}]$ is specified in Moreira et al.¹¹ as $[15mm^2, 3689mm^2]$. The resizing factor R is 4 since the original mammograms are sub-sampled with a two-level wavelet transform. Mask R-CNN training is initialized using the ‘mask_rcnn_balloon’ pre-trained model²¹. The ResNet101²² is used as the Mask R-CNN backbone. The image resize mode in Mask R-CNN is set to ‘square’ and images are resized into 1024×1024 . Images in training and validation sets are augmented in one way randomly chosen from flipped up/down, left/right and rotated in 90° , 180° , 270° . All layers in the network are then trained through 10 epochs, with 100 training and 10 validation steps in each epoch, which takes around 10 minutes. The training is repeated 5 times and the model with the lowest sum of train and validation loss among all epochs is selected for testing. Except for the parameter settings mentioned above, the rest of the parameters all remain the same as the default values in the original Mask R-CNN code²¹. A comparison experiment using grayscale mammograms is also carried out. A detection is regarded as a true positive (TP) if it has a Dice similarity index (DSI)²³ no less than 0.2 to the ground truth, similar to previous studies^{19,20}. The training of Mask R-CNN is carried out on a Dell EMC PowerEdge R740 server with 384GB DDR4 RAM and two NVIDIA Tesla V100 16GB accelerator units.

III. Results

The free response operating characteristic (FROC) curves of the testing performance using pseudo-color mammograms and grayscale mammograms with Mask R-CNN are shown in Figure 2. The proposed method achieves an average true positive rate (TPR) of 0.90 at 0.9 false positive per image (FPI) as marked with a red dot on Figure 2, while using grayscale mammograms with Mask R-CNN has a FPI of 1.9 at the same TPR as marked with a blue dot on Figure 2. The partial area under the FROC curve (AUFC)²⁴ is 0.90 in the FPI range of [0,5]. The average DSI for mass segmentation is 0.88 ± 0.10 . The detection and segmentation takes approximately 20.4 seconds per image on average.

Several detection and segmentation examples on the pseudo-color images are shown in Figure 3. If a lesion is relatively small and lands in the size range of scale 1, it will have a higher intensity in the G channel and appears to be more yellow on the pseudo-color mammogram as shown in Figure 3 (a~c). If a lesion is relatively large and lands in the size range of scale 2, it will have a higher intensity in the B channel and appears to be more purple on the pseudo-color mammogram as shown in Figure 3 (d,e).

Table 1 shows the overall performance comparison between the proposed pseudo-color image & Mask R-CNN, grayscale image & Mask R-CNN and several state-of-the-art methods. Li et al.⁸ only focuses on mass detection and Zhu et al.²⁵ only focuses on mass segmentation on manually extracted regions of interest. Dhungel et al.⁶ and Min et al.¹³ both presented detection and segmentation results. These two studies^{6,13} are evaluated on the same training, validation and testing sets of INbreast mammograms as the proposed method.

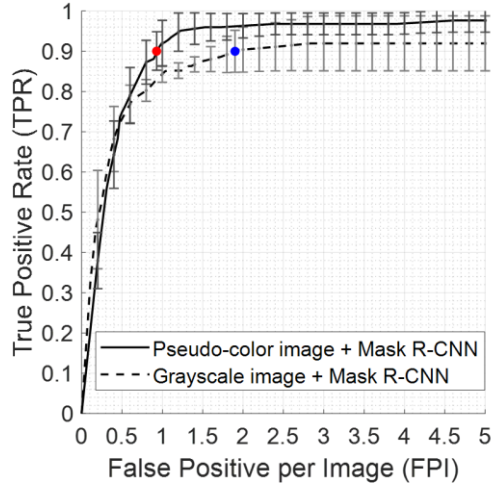


Figure 2. FROC curves for the proposed method using pseudo-color images and grayscale images with Mask R-CNN. The red dot marks an average TPR of 0.9 at 0.9 FPI using pseudo-color mammograms and the blue dot marks an average TPR of 0.9 at 1.9 FPI using grayscale mammograms.

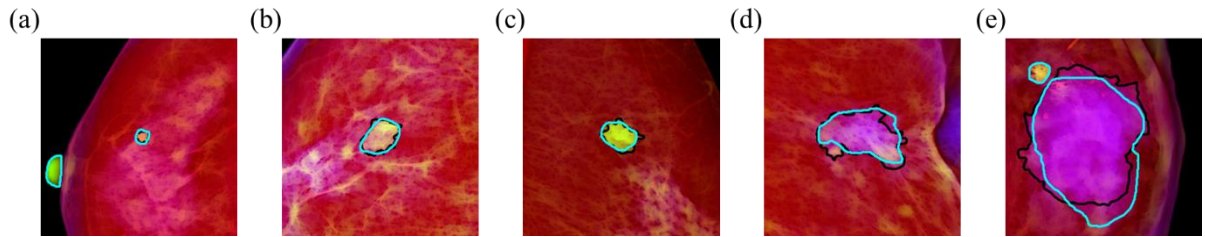


Figure 3. Detection and segmentation examples using pseudo-color images and Mask R-CNN. The black lines represent the annotation of the lesions. The cyan lines represent the segmentation of the detected regions.

IV. Discussion

The proposed method outperforms the state-of-the-art methods in mass detection and segmentation. It can perform detection and segmentation simultaneously and does not require hand-crafted features. Figure 3 showed that the MMS can sift out mass-like mammographic patterns and provide color contrast between the lesion and background tissue, which benefits

the detection and segmentation of the lesion as shown in result section. It can be observed in Figure 2 and Table 1 that the proposed method using pseudo-color images achieves a higher detection and segmentation performance than using grayscale images. In future work, we would like to explore if the pseudo-color mammograms can also improve the detection/segmentation performance when paired up with different CNN architectures.

Table 1. Mass detection and segmentation performance comparison between the proposed and several state-of-the-art methods. GM stands for grayscale mammogram and PCM stands for pseudo-color mammogram.

Methodology	Dataset	AUFC	TPR	FPI	DSI	Runtime
Li et al. ⁸	Private	--	0.90	1.9	--	--
Zhu et al. ²⁵	INbreast	--	--	--	0.91	--
Dhungel et al. ⁶	INbreast	0.83	0.90 ± 0.02	1.3	0.85 ± 0.02	39.2s
Min et al. ¹³	INbreast	0.90	0.90 ± 0.06	0.9	0.86 ± 0.08	>60s
GM & Mask R-CNN	INbreast	0.85	0.90 ± 0.05	1.9	0.87 ± 0.09	2.9s
PCM & Mask R-CNN	INbreast	0.90	0.90 ± 0.05	0.9	0.88 ± 0.10	20.4s

Compared with previous studies in Table 1, this work shows detection performance comparable to Min et al.¹³ with a higher segmentation performance. Dhungel et al.⁶ proposed a semi-automatic method with a more complex architecture, containing separate detection and segmentation stages with multiple DL networks. It requires users to manually remove FP detections before performing segmentation. Dhungel et al.⁶ and Min et al.¹³ both require hand-crafted features and a post-processing stage, while the proposed method does not. Our method achieves the highest average DSI, however at a higher variance. With a larger dataset, the performance stability can potentially be improved. In future work, we would like to evaluate our method on larger mammographic datasets, and investigate the method's

capability of identifying different types of lesions. The proposed CAD system has a shorter runtime compared with the two previous studies^{6,13}. As to the other two studies, Li et al.⁸ and Zhu et al.²⁵, they either only perform mass detection or segmentation.

V. Conclusion

In this work, we proposed an integrated mammographic mass detection and segmentation system that contains a novel pseudo-color image generation stage based on morphological sifting. The pseudo-color mammograms provide color contrast between the masses and the background tissue, which significantly improves the detection and segmentation performance of the Mask R-CNN compared with using conventional grayscale mammograms. The proposed CAD system does not require hand-crafted features or users to remove FP detections before performing segmentation. Compared with the state-of-the-art methods, the system achieves favorable performance in both mass detection and segmentation at a shorter execution time in a simple framework. By directly delineating the masses during detection, the proposed method has the potential of better assisting the radiologists in analyzing the morphology of the masses for further interpretation.

Reference

1. Jemal A, Bray F, Center MM, Ferlay J, Ward E, Forman D. Global cancer statistics. *CA Cancer J Clin.* 2011;61(2):69-90.
2. Dromain C, Boyer B, Ferré R, Canale S, Delaloge S, Balleyguier C. Computed-aided diagnosis (CAD) in the detection of breast cancer. *Eur J Radiol.* 2013;82(3):417-423.
3. Oliver A, Freixenet J, Martí J, Pérez E. A review of automatic mass detection and segmentation in mammographic images. *Med Image Anal.* 2010;14(2):87-110.

4. Schnabel JA, Giger ML, Karssemeijer N. Breast Image Analysis for Risk Assessment, Detection, Diagnosis, and Treatment of Cancer. *Annu Rev Biomed Eng.* 2013;15:327-357.
5. Li W, Zhao R, Xiao T, Wang X. Deepreid: Deep filter pairing neural network for person re-identification. Paper presented at: Proceedings of the IEEE Conference on Computer Vision and Pattern Recognition 2014.
6. Dhungel N, Carneiro G, Bradley AP. A deep learning approach for the analysis of masses in mammograms with minimal user intervention. *Med Image Anal.* 2017;37:114-128.
7. Al-antari MA, Al-masni MA, Choi M-T, Han S-M, Kim T-S. A fully integrated computer-aided diagnosis system for digital X-ray mammograms via deep learning detection, segmentation, and classification. *Int J Med Inform.* 2018;117:44-54.
8. Li Y, Chen H, Zhang L, Cheng L. Mammographic mass detection based on convolution neural network. Paper presented at: 2018 24th International Conference on Pattern Recognition (ICPR); 20-24 Aug. 2018, 2018.
9. Li H, Chen D, Nailon WH, Davies ME, Laurenson D. Improved Breast Mass Segmentation in Mammograms with Conditional Residual U-Net. Paper presented at: Image Analysis for Moving Organ, Breast, and Thoracic Images; 2018//, 2018; Cham.
10. He K, Gkioxari G, Dollár P, Girshick R. Mask r-cnn. Paper presented at: Computer Vision (ICCV), 2017 IEEE International Conference on 2017.
11. Moreira IC, Amaral I, Domingues I, Cardoso A, Cardoso MJ, Cardoso JS. INbreast: toward a full-field digital mammographic database. *Acad Radiol.* 2012;19(2):236-248.
12. Source code on GitHub. <https://github.com/Holliemin9090/Mammographic-mass-CAD-via-pseudo-color-mammogram-and-Mask-R-CNN>. Published 2019. Accessed.

13. Min H, Chandra SS, Crozier S, Bradley AP. Multi-scale sifting for mammographic mass detection and segmentation. *Biomedical Physics & Engineering Express*. 2019;5(2).
14. Daubechies I. *Ten lectures on wavelets*. Vol 61: Siam; 1992.
15. Ren S, He K, Girshick R, Sun J. Faster r-cnn: Towards real-time object detection with region proposal networks. Paper presented at: Advances in neural information processing systems2015.
16. Long J, Shelhamer E, Darrell T. Fully convolutional networks for semantic segmentation. Paper presented at: Proceedings of the IEEE conference on computer vision and pattern recognition2015.
17. Girshick R. Fast r-cnn. Paper presented at: Proceedings of the IEEE international conference on computer vision2015.
18. Dubitzky W, Granzow M, Berrar DP. *Fundamentals of data mining in genomics and proteomics*. Springer Science & Business Media; 2007.
19. Dhungel N, Carneiro G, Bradley AP. Automated Mass Detection in Mammograms using Cascaded Deep Learning and Random Forests. Paper presented at: 2015 International Conference on Digital Image Computing: Techniques and Applications (DICTA)2015.
20. Min H, Chandra SS, Dhungel N, Crozier S, Bradley AP. Multi-scale mass segmentation for mammograms via cascaded random forests. Paper presented at: 2017 IEEE 14th International Symposium on Biomedical Imaging (ISBI 2017)2017.
21. Matterport. Mask R-CNN. https://github.com/matterport/Mask_RCNN. Published 2018. Accessed.

22. He K, Zhang X, Ren S, Sun J. Deep residual learning for image recognition. Paper presented at: Proceedings of the IEEE conference on computer vision and pattern recognition2016.
23. Dice LR. Measures of the amount of ecologic association between species. *Ecology*. 1945;26(3):297-302.
24. Chakraborty DP. Validation and Statistical Power Comparison of Methods for Analyzing Free-response Observer Performance Studies. *Acad Radiol*. 2008;15(12):1554-1566.
25. Zhu W, Xiang X, Tran TD, Hager GD, Xie X. Adversarial deep structured nets for mass segmentation from mammograms. Paper presented at: 2018 IEEE 15th International Symposium on Biomedical Imaging (ISBI 2018); 4-7 April 2018, 2018.